Features of dynamic fracture of ultrafine-grained aluminum alloy AMg4.5

© A.D. Evstifeev[1,2]

[1] Research Institute of Mechanics, Lobachevsky State University of Nizhny Novgorod,
603022 Nizhny Novgorod, Russia
[2] St. Petersburg State University,
199034 St. Petersburg, Russia
e-mail: ad.evstifeev@gmail.com

The features of the fracture of the aluminum alloy AMg4.5 under dynamic tension according to the Kolsky methods using Split-Hopkinson pressure bar are considered. Experimental and theoretical data of strength characteristics of the alloy in the initial coarse-grained and ultrafine-grained states are presented. It is shown that the high degree of deformation of the material obtained in the process of severe plastic deformation by torsion under high pressure has a negative effect on the dynamic strength of the material.

Keywords: dynamic strength, incubation time criterion, Split-Hopkinson pressure bar, severe plastic deformation.

Introduction

Application of aluminum alloys in industry is due to increased strength and performance characteristics. In addition, application of this metal greatly facilitates the weight of all structures. For example, alloys of the $Al-Mg$ system are characterized by a combination of satisfactory strength and good ductility. They also have the potential to improve strength properties through work hardening [1]. As a promising direction regarding deformation processing of materials, which allows to form unique properties in a material, the methods of severe plastic deformation (SPD) can be singled out. In recent years, a plenty of studies have been carried out on pure aluminum and alloys based on it, subjected to SPD [2–8]. It was shown that SPD allows to increase the strength of the material due to grain refinement and the formation of a special structure. In some cases, materials with increased and even outstanding values of strength and plasticity were obtained [9,10]. Meanwhile, the vast majority of experiments confirming the outstanding properties of new materials were obtained under quasi-static loading conditions. Dynamic loading for this type of materials is practically not reviewed.

A peculiarity of dynamic testing is the high variability of results depending on the loading rate [11–17], as well as other factors affecting the material characteristics. Studying the literature shows that the dynamic strength and failure processes of nanomaterials in a wide range of strain rates are not well understood, and the available results are contradictory. For example, there are reports of higher impact toughness of UFG materials than their coarse-grained counterparts [18,19], and vice versa [20].

This paper presents the results of experimental studies of the deformation and strength properties of the AMg4.5 aluminum alloy in the initial coarse-grained (CG) and ultrafine-grained (UFG) states under various speed loading conditions. Dynamic tensile experiments were performed on an impact unit adapted to testing small samples according to the Kolsky method using split Hopkinson rods.

1. Material and research techniques

This paper reviews the aluminum alloy AMg4.5 (Al–4.56Mg–0.46Mn–0.32Fe–0.21Si (wt.%)). The starting material was in the as-cast condition. The structure was modified by high pressure torsion (HPT) on a Walter-Klement GmbH press. Primary HPT treatment for 10 turns was carried out at room temperature under a pressure of 6 GPa. As a result of deformation, disks 20 mm in diameter and 1.6 mm thick were formed. The true logarithmic degree of material deformation at the middle of the disk radius was $e \approx 5.5$ [21].

The microstructure of the material in the UFG state was studied by transmission electron microscopy (TEM) on a Zeiss Libra 200FE microscope.

Mechanical tensile tests were performed at a constant strain rate $5 \cdot 10^{-4}\,\text{s}^{-1}$ on samples with geometric dimensions of the working part 5 mm in length and 2 mm in width. According to the results of mechanical tests, the average values of conditional yield stress ($\sigma_{0.2}$) corresponding to 0.2% of deformation, ultimate strength (σ_{UTS}), ultimate elongation (δ) were determined. The fractography of the sample surface destroyed under uniaxial tension was performed by scanning electron microscopy (SEM) on a Zeiss AURIGA Laser microscope.

Dynamic tension experiments were carried out according to the Kolsky method using split Hopkinson rods [22,23] on samples similar to those used under quasi-static loading conditions. The unit consists of a pneumatic loading device with a caliber with the gage of 27 mm, striker 400 mm

long, split Hopkinson pressure bars with the diameter of 16 mm and loading bar length of 3000 mm, as well as a measuring bar — 1500 mm [24]. The striker is accelerated by compressed air supplied by the compressor into the chamber, pressure is monitored by a pressure gage. Variation of the impactor speed is carried out by changing the pressure from 3 to 6 bar. After the valve opens, the striker accelerates and hits the anvil rigidly connected to the loading bar. A tension pulse is generated in the loading bar and is recorded by resistive strain sensors. The pulse passing through the specimen is similarly recorded on the supporting bar. As the sample has a short length, and the time of wave propagation along the length of the sample is significantly less than the duration of the loading pulse, the stress-strain state of the sample is close to the fixed one under conditions of quasi-static loading, but proceeding at high strain rates. Thus, there is an opportunity to calculate the stresses and strains in the sample using the obtained impulses [23].

The threshold quantity to characterize the sample failure under impact loading in this paper is the dependence of the maximum breaking stress on stress increase rate. A procedure for test data analysis is provided in [24]; it includes an automated algorithm for experimental data array digitization and estimation of the rate dependence of strength.

2. Experimental results and discussion

The tensile strength of the material after HPT treatment for 10 turns increased relative to the strength of the initial state from 240 to 725 MPa. The offset yield strength increased from 120 to 725 MPa, the ultimate elongation decreased from 11% to values close to 0%. Diagrams of deformation of materials in the initial state and after HPT treatment for 10 turns are shown in Fig. 1. The high strength of the material after HPT is due to the Hall−Petch [25,26]
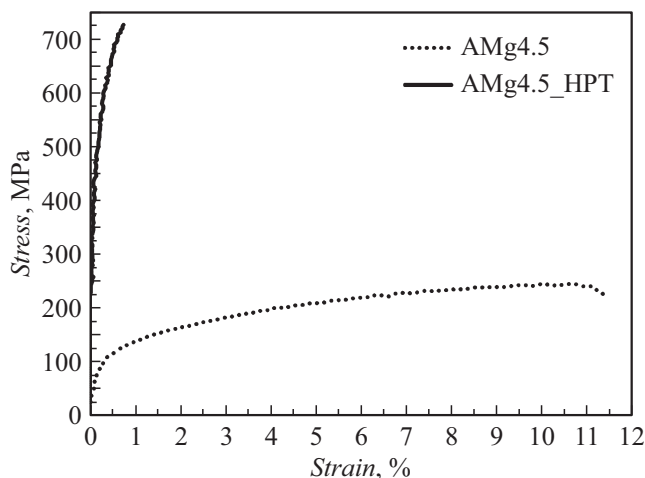

Figure 1. Stress−strain curves for tensile testing of the material in the initial state and after HPT treatment for 10 turns at a strain rate of $5 \cdot 10^{-4} \, \mathrm{s}^{-1}$.

strengthening. The average grain size is 110 nm, which is significantly less than the average grain size 41 μm for the material in the initial CG state. The average grain size was determined by the secant method using a sample of more than 250 grains.

The specimens after HPT treatment fractured brittlely, practically without plastic deformation (Fig. 2), while the material in the initial state is characterized by extensive plastic deformation zones with a strong relief structure on the failure surface (Fig. 3).

Experiments on dynamic tension using a setup that implements the scheme of split Hopkinson rods showed that an increase in the strain rate for an aluminum alloy in the initial state leads to an increase in the threshold strength characteristics (Fig. 4) by 15−30% relative to the values obtained in conditions of quasi-static loading. The alloy after HPT treatment for 10 turns, on the contrary, is characterized by a decrease in the threshold strength characteristics by 5−20% relative to the values obtained under quasi-static loading conditions. The experimental conditions for the material in the CG and UFG states were identical.

The incubation time criterion is well applicable [27] to analyze the strength characteristics of the material in the initial state:

$$\frac{1}{\tau} \int_{t-\tau}^{t} \frac{\sigma(s)}{\sigma_{UTS}} \, ds \leq 1, \tag{1}$$

where t — time, σ — dependence of breaking stress on time, σ_{UTS} — ultimate tensile strength under quasi-static loading, τ — incubation time of failure accountable for material dynamic strength. Under the condition of a constant stress growth rate $\dot{\sigma}$ in the sample up to the moment of failure or the start of irreversible deformation, the rate dependence of the critical stress level can be analytically calculated using the following formula:

$$\sigma_*(\dot{\sigma}) = \begin{cases} \sigma_{UTS} + \frac{\tau}{2}\dot{\sigma}, & \dot{\sigma} \leq \frac{2\sigma_{UTS}}{\tau}, \\ \sqrt{2\sigma_{UTS}\tau\dot{\sigma}}, & \dot{\sigma} > \frac{2\sigma_{UTS}}{\tau}. \end{cases} \tag{2}$$

With the help of the least squares method (LSM) the optimal values of the parameter τ can be calculated, which minimize the root-mean-square deviation of the calculated dependence (2) on the experimental points, shown in Fig. 4. The calculated dependence of the breaking threshold stress on the rate of stress growth for the AMg4.5 alloy in the initial state is shown in Fig. 4. $\sigma_{UTS} = 240 \, \mathrm{MPa}$ and $\tau = 10 \, \mu$s were used as material parameters.

For experimental data on the dynamic tension of the aluminum alloy AMg4.5 after HPT treatment for 10 turns, as part of the applied failure criterion, it is impossible to construct a calculated dependence due to the embrittlement of the material when a certain threshold in terms of the stress growth rate is exceeded and, thereby, a decrease in strength characteristics relative to the threshold values obtained under conditions of quasi-static loading. Despite this, it can be seen that the experimental points in the
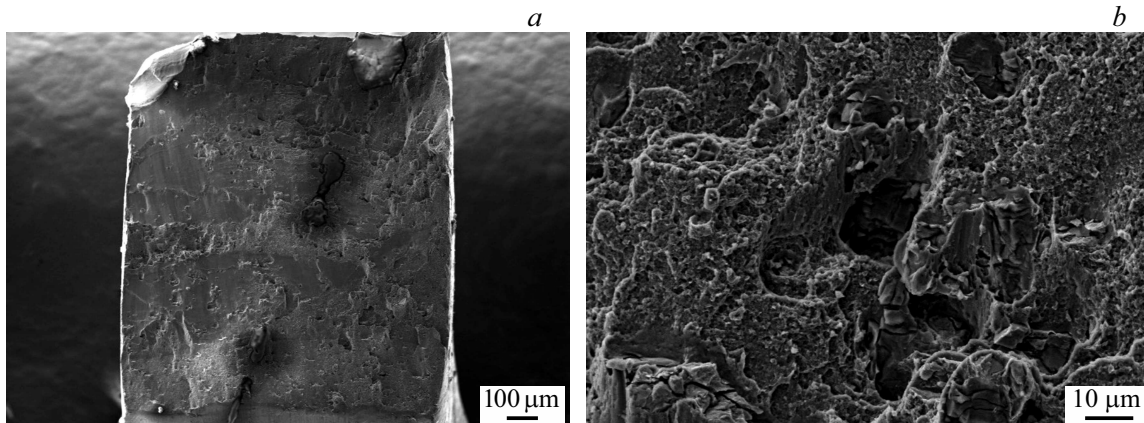
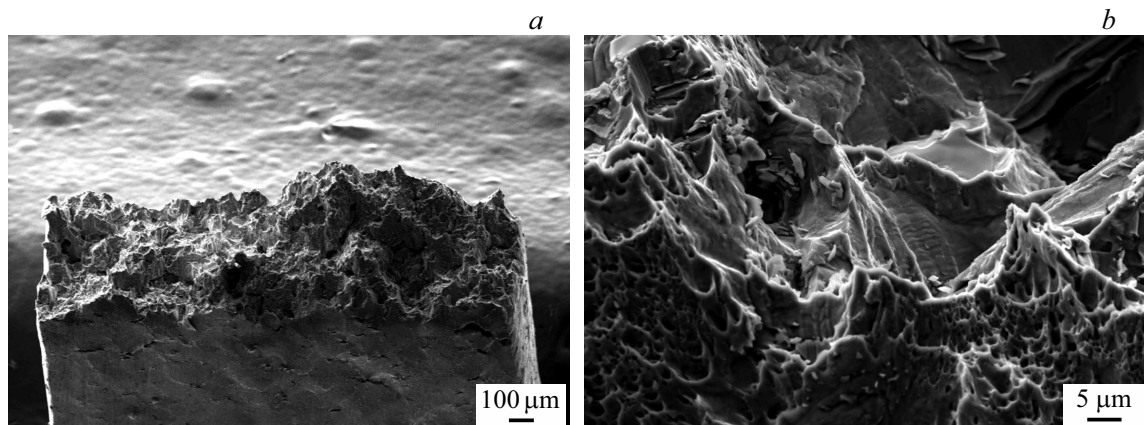**Figure 2.** SEM data. Failure surface of AMg4.5 alloy after HPT treatment for 10 turns.

Figure 3. SEM data. Failure surface of the AMg4.5 alloy in the initial CG state.
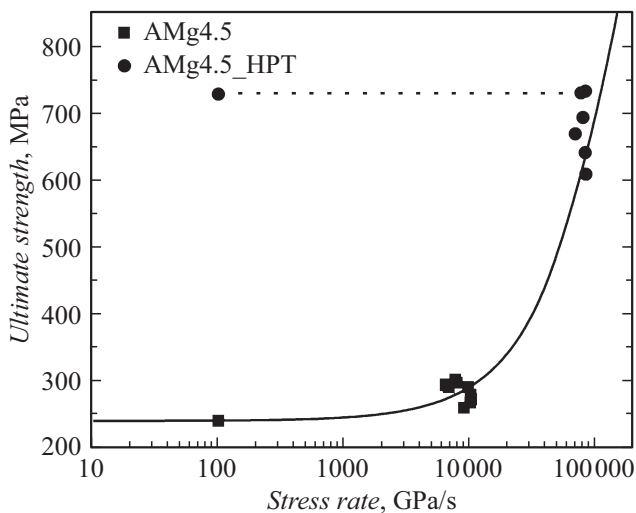

Figure 4. Experimental dependences of the maximum tensile strength on the stress growth rate of the AMg4.5 alloy in the initial CG state and after HPT treatment for 10 turns. The calculated curve is constructed according to formula (1) using the parameters $\sigma_{UTS} = 240$ MPa and $\tau = 10 \mu$s for the material in the CG state.

dynamic area are in good compliance with the calculated curve constructed for AMg4.5 in the initial CG state for higher values of the stress growth rate. This fact allows to make an assumption about similar deformation mechanisms for the material in the UFG state and the material in the CG state at high strain rates. For the AMg4.5 alloy in the initial CG state, it is impossible to achieve the stress growth rates, and thus the threshold strength values obtained in the impact testing of the alloy in the UFG state, due to the high ductility of the material. I.e., it has a low inertia and is able to relax the emerging stresses in a short period of time due to the transition of elastic deformation into plastic. The material obtained by SPD, on the contrary, is characterized by an almost complete lack of plasticity, which is expressed in the impossibility of activating the processes of dynamic hardening. This peculiarity results in the failure of the material when the characteristic threshold values of the stress growth rate are reached, at which the material, under certain conditions, would be able to demonstrate an increase in the threshold strength characteristics with an increase in the strain rate.

Analyzing the failure surface of the AMg4.5 alloy in the initial CG state under dynamic tension (Fig. 5), the
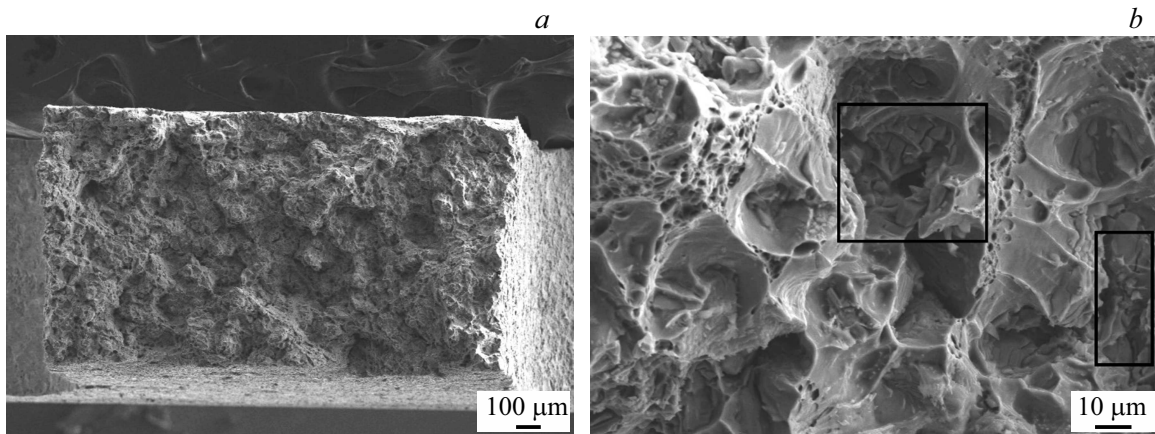
Figure 5. SEM data. Failure surface of the AMg4.5 alloy in the initial CG state under dynamic tension.
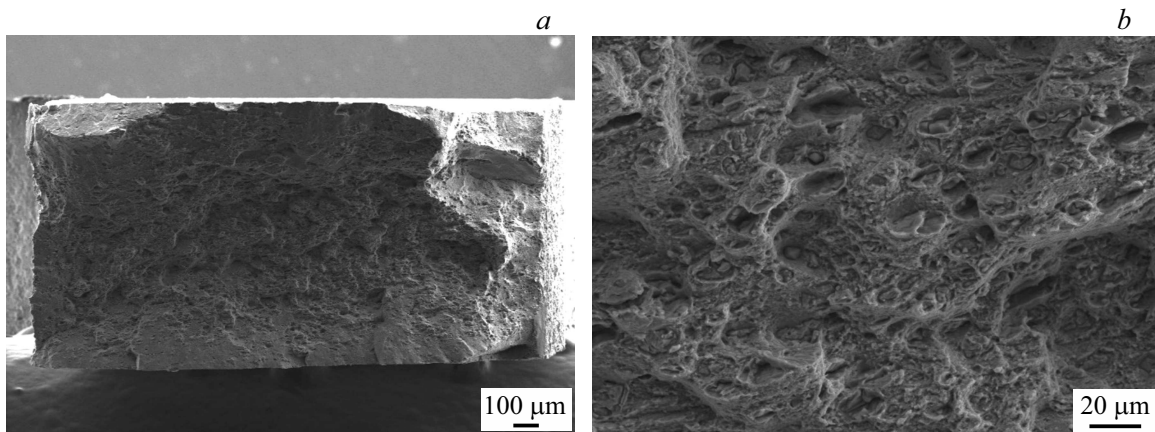

Figure 6. SEM data. Failure surface of AMg4.5 alloy after HPT treatment for 10 turns, under conditions of dynamic tension.
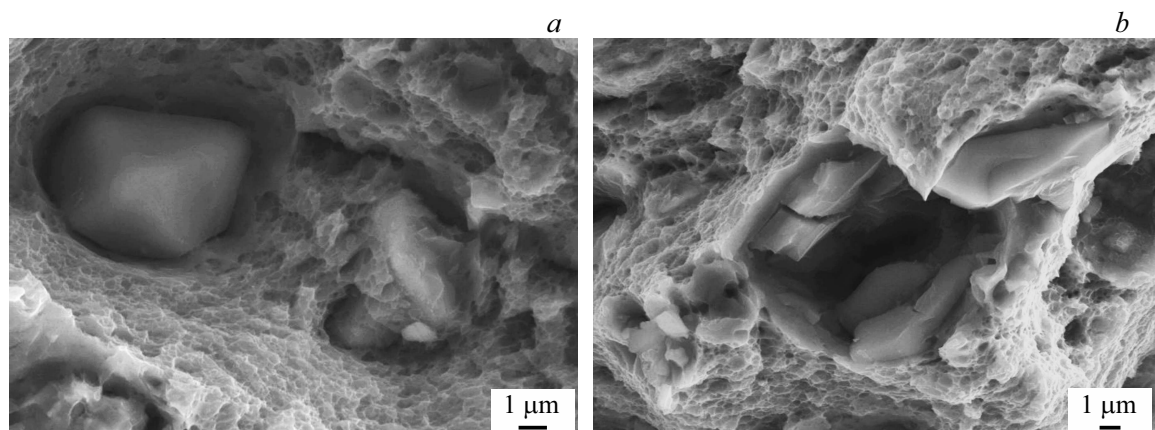

Figure 7. SEM data. Failure surface of AMg4.5 alloy after HPT treatment for 10 turns, under conditions of dynamic tension.

heterogeneity can be noted in the distribution of the shape and size of micropores. Neighboring micropores grow together and grow to a larger size in local areas. In some areas on the failure surface, the presence of microcracking areas can be noted (Fig. 5, *b*), marked by a frame, which is not observed under quasi-static loading conditions (Fig. 3). This indicates the activation of a limited number of micropore nucleation sites. Meanwhile, the areas of plastic deformation make up a large part of the failure surface.

Failure surface of AMg4.5 alloy after HPT treatment for 10 turns, under conditions of dynamic tension. (Fig. 6) is

characterized by brittle failure. On the failure surface, it is possible to specify areas of material with chipping, which are local stress concentrators in the case of dynamic tension. In addition, failure can be characterized as intergranular (Fig. 7), since the pits on the sample surface have a uniform pattern with characteristic sizes of $100-300$ nm, which corresponds to the grain size in the material after HPT processing by 10 turns.

The decrease in the threshold strength values for a material with an UFG structure in the area of dynamic loads compared to the quasi-static loading mode can be explained both by the presence of stress concentrators in the form of particles of secondary phases [28], and by different scale levels of failure. Since impact tension in the unit using the scheme of split Hopkinson rods is characterized by a linearly increasing load with time, the presence of stress concentrators in the material with an UFG structure in the form of secondary phases and the tendency of the material to brittle failure allows failure to be realized in the local volume of the material in the environment of the stress concentrator at stresses less than the threshold, determined under conditions of quasi-static loading.

Conclusion

Using the example of aluminum alloy AMg4.5, the paper proposes an approach based on HPT treatment to improve the strength characteristics of the material. The tensile strength of the material was increased from 240 to 725 MPa under quasi-static loading, but in this case there was a complete loss of plasticity.

In experiments on dynamic tension using a unit that implements the Kolsky method using split Hopkinson rods, the aluminum alloy in the CG state showed the effect of hardening with increasing strain rate. The alloy in the UFG state, on the contrary, with an increase in the rate of application of the load, was destroyed at stresses lower than its static strength.

Using the incubation time criterion for experimental data in the area of quasi-static and dynamic loading of the alloy in the CG state, the material parameters were determined and the calculated dependences of the maximum tensile strength on the stress growth rate were plotted. A good agreement between the calculated curve and the experimental points was obtained.

It is shown that a high degree of material deformation obtained in the process of severe plastic deformation of the AMg4.5 alloy has a negative effect on the dynamic strength of the material. With an increase in the rate of application of the load, the material with the UFG structure becomes brittle, however, the experimental points in the dynamic area are in good compliance with the calculated curve constructed for AMg4.5 in the initial CG state.

Conflict of interest

The authors declares that he has no conflict of interest.

References

[1] L.F. Mondolfo. *Aluminum Alloys: Structure and Properties* (Elsevier, 2013)

[2] H. Miyamoto, K. Ota, T. Mimaki. Scripta Mater., **54**, 1721 (2006).

[3] B. Talebanpour, R. Ebrahimi, K. Janghorban. Mater. Sci. Eng. A, **527**, 141 (2009).

[4] I. Sabirov, M.Yu. Murashkin, R.Z. Valiev. Mater. Sci. Eng. A, **560**, 1 (2013).

[5] R.Z. Valiev, M.Yu. Murashkin, I. Sabirov. Scripta Mater., **76**, 13 (2014).

[6] A.M. Mavlyutov, I.A. Kasatkin, M.Y. Murashkin, R.Z. Valiev, T.S. Orlova. Phys. Solid State, **57**, 2051 (2015).

[7] X. Huang, N. Hansen, N. Tsuji. Science, **312**, 249 (2006).

[8] N. Kamikawa, X. Huang, N. Tsuji, N. Hansen. Acta Mater., **57**, 4198 (2009).

[9] A.M. Mavlyutov, T.A. Latynina, M.Yu. Murashkin, R.Z. Valiev, T.S. Orlova. Phys. Solid State, **59**, 1970 (2017).

[10] R.Z. Valiev, I.V. Alexandrov, Y.T. Zhu, T.C. Lowe. J. Mater. Res., **17**, 5 (2002).

[11] G.V. Stepanov, V.V. Astanin, V.I. Romanchenko, A.P. Vashchenko, V.M. Tokarev, B.D. Chukhin, Y.P. Guk. Strength Mater., **15**, 220 (1983).

[12] A.M. Bragov, A.K. Lomunov. PMTF, **5**, 168 (1988) (in Russian)

[13] A.M. Bragov, B.L. Karihaloo, Yu.V. Petrov, A.Yu. Konstantinov, D.A. Lamzin, A.K. Lomunov, I.V. Smirnov. J. Appl. Mech. Tech. Phys., **53**, 926 (2012).

[14] A.A. Gruzdkov, E.V. Sitnikova, N.F. Morozov, Y.V. Petrov. Math. Mech. Solids, **14**, 72 (2009).

[15] A.A. Gruzdkov, S.I. Krivosheev, Y.V. Petrov. Phys. Solid State, **45**, 886 (2003).

[16] G.I. Kanel, S.V. Razorenov, A.A. Bogatch, A.V. Utkin, V.E. Fortov, D.E. Grady. J. Appl. Phys., **20**, 467 (1997).

[17] G.V. Garkushin, G.I. Kanel, S.V. Razorenov. FTT, **52**, 2216 (2010) (in Russian)

[18] J.S. Liao, M. Hotta, K. Kaneko, K. Kondoh. Scr. Mater., **61**, 208 (2009).

[19] G. Purcek, O. Saray, I. Karaman, T. Kucukomeroglu. Mater. Sci. Eng. A, **490**, 403 (2008).

[20] A.A. Karimpoor, K.T. Aust, U. Erb. Scr. Mater., **56**, 201 (2007).

[21] A.P. Zhilyaev, T.G. Langdon. Prog. Mater. Sci., **53**, 893 (2008).

[22] H. Kolsky. Proc. Phys. Soc., **62**, 676 (1949).
[23] A.M. Bragov, A.K. Lomunov. Int. J. Impact. Engng. **16** (2), 321 (1995).
[24] A.D. Evstifeev, G.A. Volkov. ZhTF, **92** (2), 274 (2022) (in Russian) DOI: 10.21883/JTF.2022.02/52017.250-21
[25] E.O. Hall. Proc. Phys. Soc. B, **64**, 747 (1951).
[26] N.J. Petch. The Orientation Relationships Between Cementite and α-iron. Acta Crystallographica, **6**, 96 (1953).
[27] Yu.V. Petrov. DAN, **395** (5), 621 (2004) (in Russian)
[28] M.Y. Murashkin, N.A. Enikeev, V.U. Kazykhanov, I. Sabirov. Rev. Adv. Mater. Sci., **35**, 75 (2013).